Journal of Computational Methods in Molecular Design, 2015, 5 (1):15-26

Scholars Research Library
(http://scholarsresearchlibrary.com/archive.html)

ISSN : 2231- 3176
CODEN (USA): JCMMDA

A Quantum Chemical Analysis of the Inactivation Rate Constant of the BoNT/A LC Neurotoxin by some 1,4-Benzoquinone and 1,4-Naphthoquinone derivatives.

Juan S. Gómez-Jeria* and Andrés Robles-Navarro

Department of Chemistry, Faculty of Sciences, University of Chile. Las Palmeras 3425, Santiago 7800003, Chile

---

ABSTRACT

An investigation of the relationships between the inactivation rate constant of the BoNT/A LC neurotoxin by several 1,4-benzoquinone and 1,4-naphthoquinone derivatives was carried out. A statistically significant relationship was found (n=21, R= 0.97, F(7,13)=25.63 (p<0.000001), SD=0.20) involving local atomic reactivity indices of two oxygen atoms and a carbon one. The conditions for a high rate are presented and discussed. The suggestion that these molecules form a covalent bond with Cys-165 after the formation of the reversible ligand-site complex was tested through a docking study of all the molecules with the B monomer of the Clostridium botulinum neurotoxin serotype A light chain. It is found that Cys-165 is very far for the site of the reversible ligand-site interaction. It is suggested that His-223 is a better candidate for a covalent bond formation.

Keywords: Botulinum neurotoxin**,** BoNT/A, 1,4-benzoquinone, 1,4-naphthoquinone, chemical reactivity, irreversible inhibitors, bioterrorism, BoNT/A LC, DFT, QSAR, docking, benzoquinone, Hammett.

INTRODUCTION

US CDC classifies botulism as a category A bioweapon (the genetically-modified H5N1 virus is not classified by CDC due to the highly incorrect reasoning that nobody will produce and use it) [1-4]. Botulinum toxins are produced by the bacteria *Clostridium Botulinum* and are some of the most lethal known venoms [5, 6]. The toxin blocks the nerve's capacity to release acetylcholine, the component that relays signals from the nervous system to muscles. The result is paralysis and death. In 1939 botulinum toxins were included in Canada's biological weapons arsenal. USA, the Soviet Union, South Africa and Iraq included botulinum toxins in their arsenals. The Japanese military fed *Clostridium botulinum* cultures to prisoners of war in their secret laboratories located in Manchukuo (a pro-Japanese government was installed there with Puyi, the last Qing emperor, as the nominal regent and emperor, 1932-1945) to examine the lethal effect of the toxin. During a research on botulinum neurotoxin serotype A (BoNT/A) inhibitors it was found that some 1,4-benzoquinone and 1,4-naphthoquinone derivatives acted as irreversible inhibitors (irreversible inhibitors usually react with the enzymes and produce a covalent modification of them, so that their activity is permanently reduced. A classical example is potassium cyanide that is an irreversible inhibitor of the enzyme cytochrome C oxidase, which participates in respiration reactions in cells) of BoNT/A LC (the catalytic light chain, LC, domain of BoNT/A is a compact ball consisting of a combination of α-helices, β-sheets, and β-strands with a zinc-containing metalloprotease active site bound profoundly inside a great open cavity) [7]. The rate constant to form the inactivated enzyme-ligand complex, K_{inact} was reported. It was suggested that these irreversible inhibitors act by probably modifying Cys-165 through covalent bonding. On our hand, we have developed a formal linear relationship between the drug-enzyme (ligand-receptor) equilibrium constant, K, and the electronic structure of only the ligands [8-13]. In the case of irreversible inhibitors this equilibrium is the previous step before the covalent bond formation. In this paper, and for the first time, we present the results of a formal

quantum-chemical study relating the variation of K_{inact} with the variation of local atomic reactivity indices of a set of the abovementioned molecules.

MATERIALS AND METHODS

METHODS AND CALCULATIONS

The relationship between K_{inact} and electronic structure has the form [9]:

$$\log(K_{inact})_i = a + b\log(M_i) + c\log\left[\frac{\sigma_i}{(ABC)_i^{1/2}}\right] + d\Delta E_i \qquad (1)$$

where i denotes the i-th molecule, M_i the mass, σ_i the symmetry number and ABC the product of the molecules' moment of inertia about the three principal axes of rotation. ΔE_i is expressed as [10]:

$$\Delta E_i = \sum_j \left[e_j Q_j + f_j S_j^E + s_j S_j^N \right] + + \sum_j \sum_m \left[h_j(m) F_j(m) + x_j(m) S_j^E(m) \right] +$$
$$+ \sum_j \sum_{m'} \left[r_j(m') F_j(m') + t_j(m') S_j^N(m') \right] + \sum_j \left[g_j \mu_j + k_j \eta_j + o_j \omega_j + z_j \varsigma_j + w_j Q_j^{\max} \right] \qquad (2)$$

where Q_i is the net charge of atom *i*, S_i^E and S_i^N are, respectively, the total atomic electrophilic and nucleophilic superdelocalizabilities of Fukui et al., $F_{i,m}$ is the Fukui index of atom i in occupied (empty) MO m (m'), $S_i^E(m)$ is the atomic electrophilic superdelocalizability of atom i in MO m, etc. The total atomic electrophilic superdelocalizability (ESD) of atom i is defined as the sum over occupied MOs of the $S_i^E(m)$'s and the total atomic nucleophilic superdelocalizability (NSD) of atom i is defined as the sum over empty MOs of the $S_i^N(m')$'s. S_i^E is related to the total electron-donating capacity of atom i and S_i^N to its total electron-accepting capacity. The orbital components, $S_i^E(m)$ and $S_i^N(m')$, become significant when fine aspects of the drug-receptor interaction are needed for a more comprehensive elucidation of the physics of the interaction. The last bracket on the right side of Eq. 2 contains new local atomic indices developed in 2013 [12, 13]. μ_j, η_j, ω_j, ς_j and Q_j^{max} are, respectively, the local atomic electronic chemical potential of atom j (i.e., the midpoint of HOMO* and LUMO*), the local atomic hardness of atom j (the HOMO*-LUMO* distance), the local atomic electrophilicity of atom j, the local atomic softness of atom j and the maximal amount of electronic charge that atom j may accept [12, 13]. The application of this method to receptor binding affinities and other kinds of biological activities produced excellent results [14-39] (and references therein).

The selected molecules and their K_{inact} are shown in Fig. 1 and Table 1 [7].

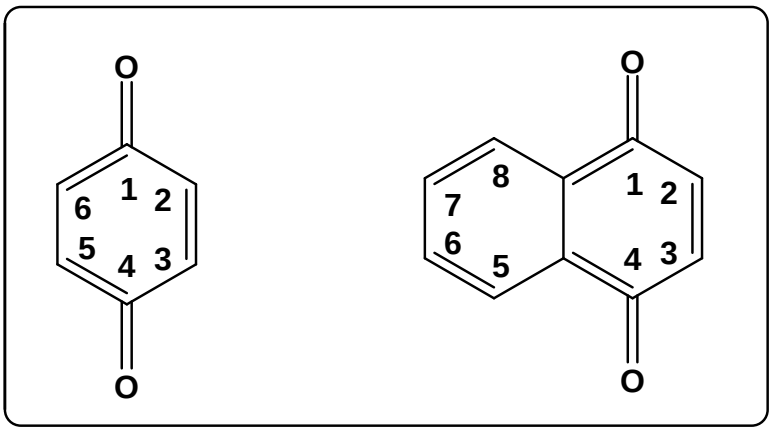

Figure 1. Molecules employed in this study (1,4-benzoquinones, BQ, and 1,4-naphthoquinones, NQ).

Table 1. Molecules and their log(K_{inact}).

Mol.	Name	log(K_{inact}) [7]
1	2,5-DiCl-BQ	3.62
2	2-Cl-BQ	3.41
3	BQ	2.93
4	2-Ph-BQ	2.69
5	2-OMe-3-Tol-BQ	2.68
6	5-OH-NQ	2.42
7	5-OCyclopentoyl-NQ	2.37
8	2-OMe-BQ	2.31
9	5-OAc-NQ	2.30
10	2-Me-BQ	2.24
11	5,8-diOH-NQ	2.04
12	5-OBn-NQ	2.00
13	NQ	2.00
14	2-(2-COOH-Et)-BQ	1.78
15	2-Me-NQ	1.74
16	5-OMe-NQ	1.69
17	6-OH-NQ	1.67
18	2-Tol-NQ	1.66
19	2,5-diOMe-3-Tol-BQ	1.61
20	2-(COOH-Me)-BQ	1.45
21	2-iPr-5-Me-BQ	1.28

Geometries were fully optimized at the B3LYP/6-31G(d,p) level of the theory with the Gaussian package of programs [40]. With the D-CENT-QSAR software we extracted from the Gaussian results all the necessary information to obtain numerical values for the local atomic reactivity indices (LARIs) [41]. All electron populations smaller than or equal to 0.01 e were considered as zero. Negative electron populations arising from Mulliken Population Analysis were corrected as usual [42]. As always we worked with the common skeleton hypothesis (CS, a group of atoms common to all molecules analyzed), stating that the variation of one or more LARIs of this common skeleton accounts for almost all the variation of K_{inact} through the series. The substituents modify the electronic structure of CS. For the case studied here the common skeleton numbering is shown in Fig. 2

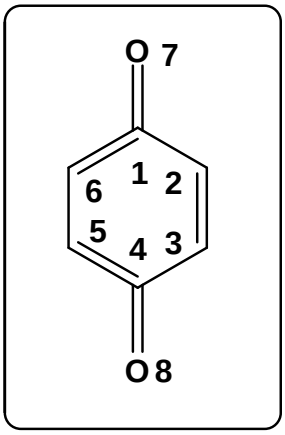

Figure 2. Common skeleton numbering.

As there are no enough molecules to solve the linear system of equations 1, we used Linear Multiple Regression Analysis (LMRA) with the Statistica software to find the most statistically significant equation [43]. The dependent variable is the logarithm of K_{inact} and the independent variables are the LARIs of the common skeleton plus log(M_i) and $\log\left[\frac{\sigma_i}{(ABC)_i^{1/2}}\right] + d\Delta E_i$.

To investigate the reversible ligand-enzyme equilibrium existing before the covalent bond formation we performed first a docking analysis of molecule 30 of Ref. [7] with the "rigid residue" and "flexible residue" options for comparison. The B monomer of the *Clostridium botulinum* neurotoxin serotype A light chain (PDB ID: 2IMB) was employed. Autodock Vina was used for the docking procedures [44]. Starting from the rigid residue results, a volume of 4 Å was defined around the ligand and all residues inside it were treated as flexible. A 30x30x30 box was

used. The molecules analyzed here were docked with the flexible residues option. The docking results were analyzed with Discovery Studio Visualizer [45].

DOCKING RESULTS

The best statistically significant equation obtained is:

$$\log(K_{inact}) = 24.59 + 1.31S_7^E - 1.32S_7^N(LUMO+2)^* + 0.16S_2^N(LUMO+2)^* + 2.01S_4^E - 0.78S_8^E(HOMO)^* + 0.85S_8^N(LUMO+2)^* + 6.11F_1(HOMO-1)^* \quad (3)$$

with n=21, R= 0.97, R^2= 0.93, adj-R^2= 0.90, F(7,13)=25.63 (p<0.000001) and a standard error of estimate of 0.20. No outliers were detected and no residuals fall outside the ±2.00 σ limits. Here, S_7^E is the total electrophilic superdelocalizability of atom 7, $S_7^N(LUMO+2)^*$ is the nucleophilic superdelocalizability of the third lowest vacant MO localized on atom 7, $S_2^N(LUMO+2)^*$ is the nucleophilic superdelocalizability of the third lowest vacant MO localized on atom 2, S_4^E is the total electrophilic superdelocalizability of atom 4, $S_8^E(HOMO)^*$ is the electrophilic superdelocalizability of the highest occupied MO localized on atom 8, $S_8^N(LUMO+2)^*$ is the nucleophilic superdelocalizability of the third lowest vacant MO localized on atom 8 and $F_1(HOMO-1)^*$ is the Fukui index of the second highest MO localized on atom 1. No terms related to the translation or rotational partition functions appear in Eq. 3.

Table 2. Beta coefficients and t-test for significance of coefficients in Eq. 3.

	Beta	**t(13)**	**p-level**
S_7^E	0.60	6.48	<0.00002
$S_7^N(LUMO+2)^*$	-0.72	-7.54	<0.000004
$S_2^N(LUMO+2)^*$	0.37	4.44	<0.0007
S_4^E	0.25	3.12	<0.008
$S_8^E(HOMO)^*$	-0.24	-2.29	<0.04
$S_8^N(LUMO+2)^*$	0.49	4.51	<0.0006
$F_1(HOMO-1)^*$	0.32	3.20	<0.007

Table 3. Matrix of squared correlation coefficients for the variables in Eq. 3.

	S_7^E	$S_7^N(LUMO+2)^*$	$S_2^N(LUMO+2)^*$	S_4^E	$S_8^E(HOMO)^*$
$S_7^N(LUMO+2)^*$	0.008	1.00			
$S_2^N(LUMO+2)^*$	0.004	0.02	1.00		
S_4^E	0.04	0.06	0.07	1.00	
$S_8^E(HOMO)^*$	0.24	0.03	0.06	0.008	1.00
$S_8^N(LUMO+2)^*$	0.004	0.29	0.0009	0.01	0.14
$F_1(HOMO-1)^*$	0.006	0.002	0.03	0.005	0.14

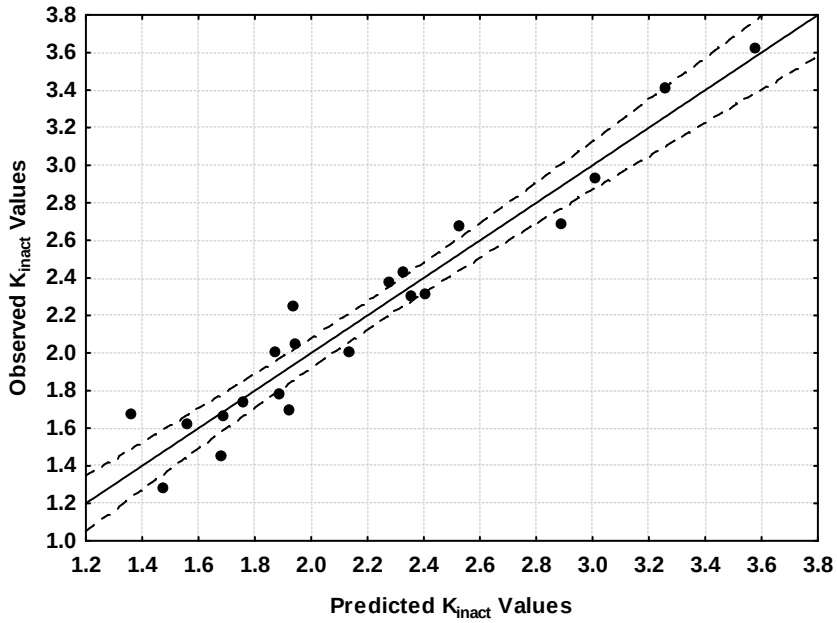

Figure 3. Plot of predicted *vs.* observed log(K_{inact}) values from Eq. 3. Dashed lines denote the 95% confidence interval.

Table 3 shows that there are no significant internal correlations between independent variables. The associated statistical parameters of Eq. 3 (Table 2) show that this equation is statistically significant and that the variation of a group of seven local atomic reactivity indices belonging to the common skeleton (Fig. 2) explains about 90% of the variation of K_{inact}. Figure 3, spanning about 2.1 orders of magnitude, shows that there is a good quality correlation of observed *versus* calculated values and that almost all points are inside the 95% confidence interval. Table 4 shows the local molecular orbital structure of some atoms appearing in Eq. 3 (nomenclature: molecule (HOMO) / (HOMO-2)* (HOMO-1)* (HOMO)*-(LUMO)* (LUMO+1)* (LUMO+2)*).

Table 4. Local Molecular Orbital structure of atoms 1, 2, 7 and 8.

Mol	Atom 1 (C)	Atom 2 (C)	Atom 7 (O)	Atom 8 (O)
1 (44)	40σ41σ42σ- 45π46π47σ	42σ43π44π- 45π46π47σ	41σ42σ43π- 45π48π52π	41σ42σ43π-45π48π52π
2 (36)	32σ33σ34σ-37π38π39σ	33σ34σ36π-37π38π39σ	34σ35π36π-37π40π45π	34σ35π36π-37π40π45π
3 (28)	25σ26σ27π-29π30π31π	26σ27π28π-29π30π31π	25σ26σ27π-29π31π32σ	25σ26σ27π-29π31π32σ
4 (48)	41σ43σ45σ-49π50π51π	44π45σ48π-49π50π52π	44π45σ46π-49π50π51π	45σ46π48π-49π52π53π
5 (60)	50σ51π55σ-61π62π65π	56σ58π60π-61π62π64π	57π58π60π-61π65π79σ	57π58π60π-61π64π65π
6 (45)	40π41σ42σ-46π47π48π	42σ43π44π-46π47π48π	43π44π45π-46π47π49π	43π44π45π-46π47π49π
7 (71)	61π66σ68σ-72π73π74π	68σ69π70π-72π73π74π	69π70π71π-72π73π77σ	69π70π71π-72π73π77σ
8 (36)	32π33σ34σ-37π38π39π	33σ34σ36π-37π38π39π	34σ35π36π-37π39π47π	34σ35π36π-37π39π47π
9 (56)	49π51σ53σ-57π58π59π	53σ54π55π-57π58π59π	54π55π56π-57π58π62π	54π55π56π-57π58π62π
10 (32)	28π29σ30σ-33π34π35π	30σ31π32π-33π34π35π	30σ31π32π-33π35π43π	30σ31π32π-33π35π40π
11 (49)	45σ46σ47π-50π51π52π	46σ47π48π-50π51π52π	47π48π49π-50π52π54π	47π48π49π-50π51π52π
12 (72)	64σ66σ67σ-73π74π75π	67σ68π69π-73π75π76π	69π71π72π-73π75π78π	69π71π72π-73π75π78π
13 (41)	36π37σ38σ-42π43π44π	38σ39π40π-42π43π44π	39π40π41π-42π43π45π	39π40π41π-42π43π45π
14 (47)	41σ43σ45σ-48π49π50π	45σ46π47π-48π49π51π	45σ46π47π-48π50π51π	45σ46π47π-48π50π51π
15 (45)	40π41σ42σ-46π47π48π	42σ43π44π-46π47π48π	43π44π45π-46π47π49π	43π44π45π-46π47π49π
16 (49)	44π45σ46σ-50π51π52π	46σ47π48π-50π51π52π	47π48π49π-50π51π53π	47π48π49π-50π51π53π
17 (45)	40π41σ42σ-46π47π50π	43π44π45π-46π48π50π	42σ43π45π-46π47π50π	42σ43π44π-46π47π50π
18 (65)	58π59σ60σ-66π67π68π	60σ61π65π-66π67π68π	61π62π63π-66π67π70π	62π63π65π-66π67π68π
19 (68)	62σ63σ64σ-69π70π73π	65π66π68π-69π70π71π	65π66π68π-69π73π90π	65π66π68π-69π70π73π
20 (43)	39σ40σ41σ-44π45π46σ	41σ42π43π-44π45π46σ	41σ42π43π-44π47π48π	40σ42π43π-44π47π48π
21 (44)	40σ41σ42σ-45π46π47π	42σ43π44π-45π46π47π	41σ42σ43π-45π47π54π	42σ43π44π-45π47π54π

RESULTS

Table 5 shows the colors associated to atoms and ligand-residue interactions.

Table 5. List of colors for docking figures analysis.

Interaction or atom	Color name	RGB
Pi-alkyl (hydrophobic)	Cotton candy	(255,200,255)
Alkyl (hydrophobic)	Cotton candy	(255,200,255)
Pi-sigma (hydrophobic)	Heliotrope	(200,100,255)
Carbon-hydrogen bond	Honeydew	(220,255,220)
Conventional H-bond	Lime	(0,255,0)
Salt bridge (attractive charge)	Orange peel	(255,150,0)
Pi-anion	Orange peel	(255,150,0)
Pi-Pi stacked	Neon pink	(255,100,200)
Pi-Pi T shaped	Neon pink	(255,100,200)
Halogen	Aqua	(0,255,255)
Attractive charge	Orange peel	(255,150,0)
Carbon-hydrogen bond, halogen	Honeydew	(220,255,220)
Pi-sulphur	Tangerine yellow	(255,200,0)
Unfavorable donor-donor	Red	(255,10,0)
Unfavorable positive-positive	Red	(255,10,0)
Pi-cation	Orange peel	(255,150,0)
Unfavorable acceptor-acceptor	Red	(255,10,0)
Amide-π stacking	Neon pink	(255,100,200)
Zn atom	Ship Cove	(124,129,175)
Sulphur atom	Sunglow	(255,200,50)

Fig. 4 shows the docking results for molecule 30 of Ref. [7].

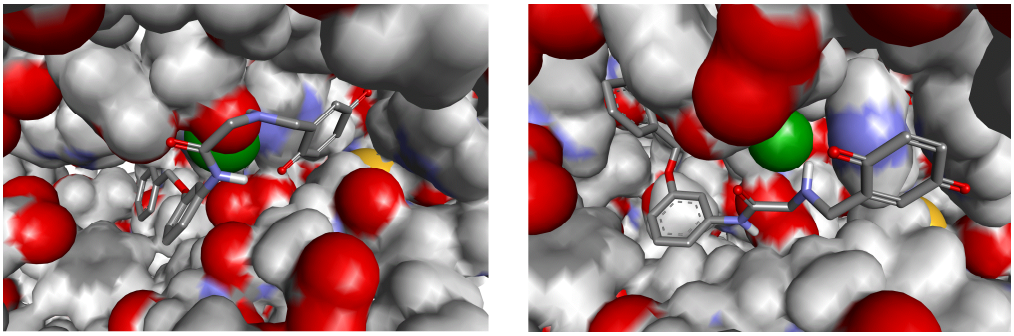

Figure 4. Docking results for molecule 30 of Ref. [7]. Left side: rigid residues option. Right side: flexible residues option.

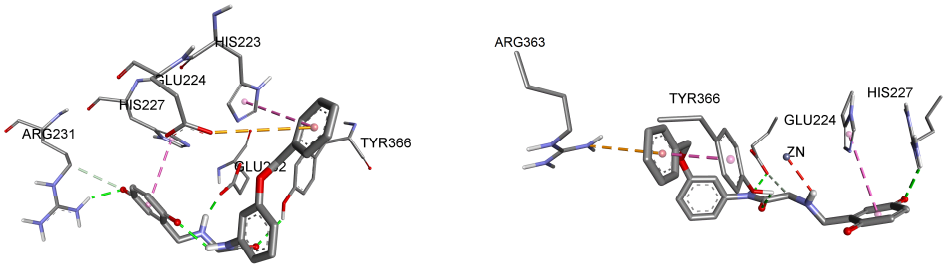

Figure 5. Ligand-site interactions for molecule 30 of Ref. [7]. Left side: rigid residues option. Right side: flexible residues option.

DISCUSSION

LRMA RESULTS

The results of the LMRA suggest that the place with which BQ and NQ form a covalent bond is the same.

The beta values (Table 2) indicate that the order of importance of variables is $S_7^N(LUMO+2)^* > S_7^E > S_8^N(LUMO+2)^* > S_2^N(LUMO+2)^* > F_1(HOMO-1)^* > S_4^E = S_8^E(HOMO)^*$. A VbV analysis shows that a high K_{inact} rate constant is associated with high values for $S_8^E(HOMO)^*$ and $F_1(HOMO-1)^*$, and

with small values for S_4^E and S_7^E. The conditions for the orbital nucleophilic superdelocalizabilities will be discussed below. $S_8^E(HOMO)*$ will not be discussed because the associated t and p level results for this index preclude a precise interpretation. Atom 1 is a carbon atom (see Fig. 2). $(HOMO-1)_1^*$ is a σ MO in all but one molecule (Table 4). A high value for this index suggests that a high value for K_{inact} is associated with a high σ electron population on this MO and possible also in $(HOMO)_1^*$. Small values for S_4^E (a C atom of the 4 position, Fig, 2) and S_7^E (the oxygen atom bonded to position 1, Fig. 2) indicate that these atoms should behave as bad electron donors. In the case of the orbital nucleophilic superdelocalizabilities, and considering together their numerical values (positive or negative) and the sign accompanying them in Eq. 3, it is possible to reason as follows. Atom 7 is the oxygen atom bonded to position 1 in Fig. 2. $(LUMO+2)_7^*$ is a π MO in almost all molecules (Table 4). For this case it is necessary that the corresponding eigenvalue shifts upwards in the energy axis, making $(LUMO+2)_7^*$ not available for electron acceptance. This is fully compatible with the condition imposed to S_7^E. Carbon atom 2 corresponds to the position 2 in Fig. 2. $(LUMO+2)_2^*$ is a π MO in almost all the molecules (Table 4). For a high value of K_{inact} the value of the eigenvalue of $(LUMO+2)_2^*$ should be shifted downwards making this OM more prone to receive electrons. It is intended that $(LUMO+1)_2^*$ and $(LUMO)_2^*$ also participate in the interaction(s). Oxygen atom 8 corresponds to the position 8 in Fig. 2 $(LUMO+2)_8^*$ is a π MO in almost all the molecules (Table 4). Here, for a high value of K_{inact} the value of the eigenvalue must also be shifted downwards making $(LUMO+2)_8^*$ more reactive. $(LUMO+1)_8^*$ and $(LUMO)_8^*$ are also involved in the interaction(s). The above suggestions are displayed in Fig. 6. The encircled atoms are the most important contributors to Eq. 3 (Table 2).

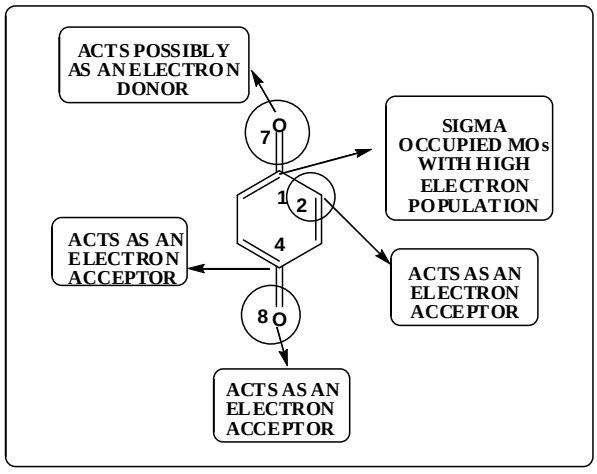

Figure 6. Known conditions for high K_{inact} values.

DOCKING RESULTS

We can see that the results presented in the left side of Fig. 4 are almost coincident with those of Ref. [7]. The flexible residues results are different (Fig. 4, right side). The differences in the kinds of ligand-site interactions are shown in Fig. 5 (see Table 5). Notice that His-227 is common to both results. The thiol of cysteine is the most important redox-active and nucleophilic functional group in biological systems [46]. This supports the suggestion that Cys-165 could be the target for the formation of a covalent bond between the molecules and the site [7]. But it is well known that also the imidazole group in histidine and the terminal amino group in lysine and are also targets for quinones [7, 47]. The presence of histidine residues in the binding site and the acceptance of the model stating that first the molecules interact weekly with the site and after form a covalent bond with a residue prompted us to examine the distance between the weakly bonded molecules to Cys-165 and His-227. Figures 7 to 12 show the results.

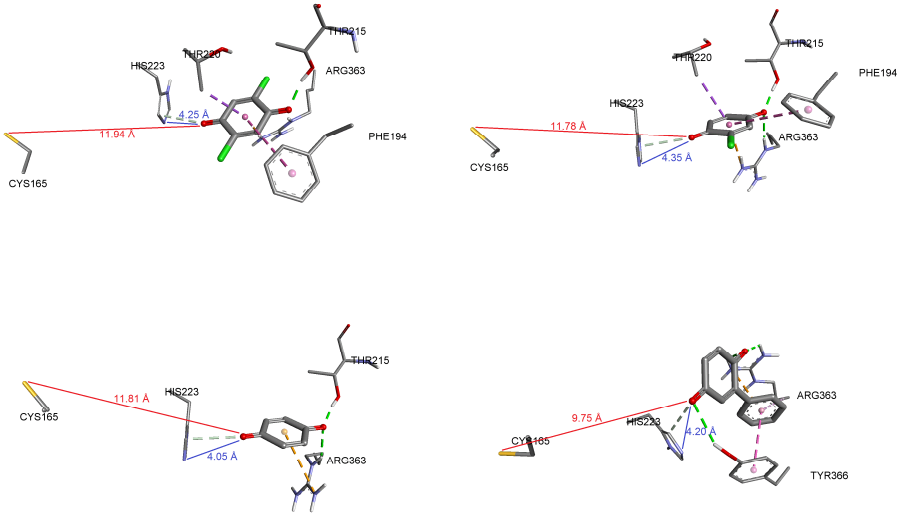

Figure 7. Molecules 1 (upper left), 2 (upper right), 3 (lower left) and 4 (lower right) docked to the binding site.

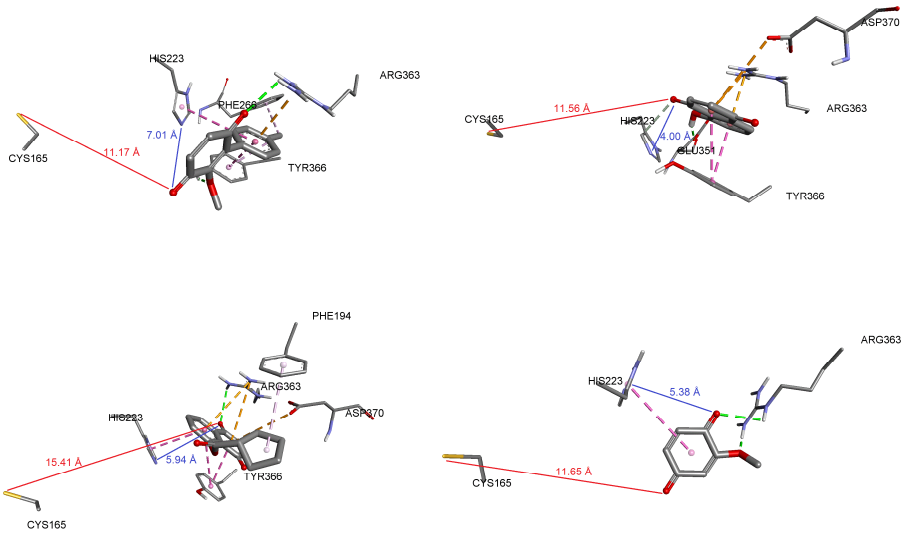

Figure 8. Molecules 5 (upper left), 6 (upper right), 7 (lower left) and 8 (lower right) docked to the binding site.

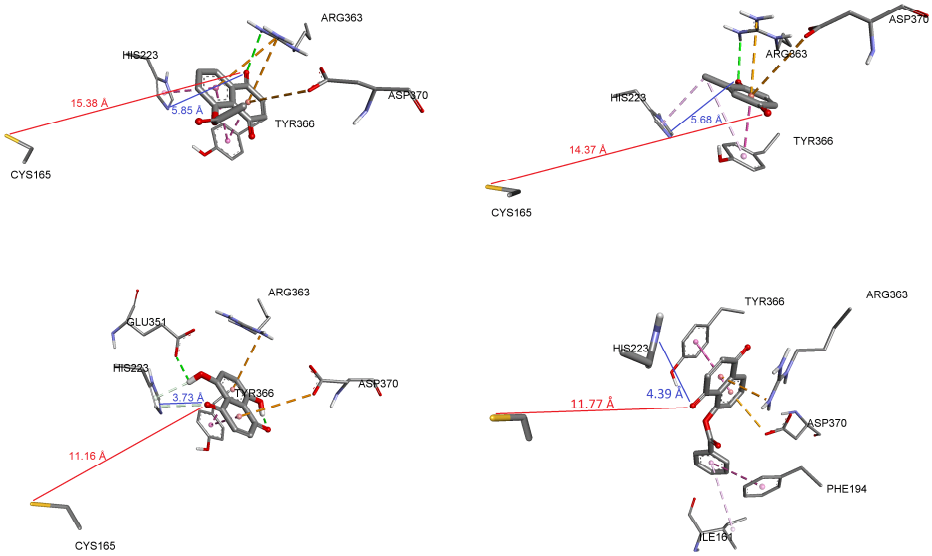

Figure 9. Molecules 9 (upper left), 10 (upper right), 11 (lower left) and 12 (lower right) docked to the binding site.

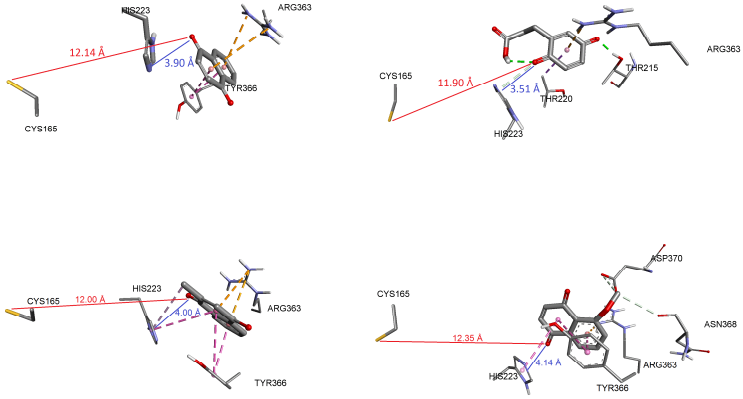

Figure 10. Molecules 13 (upper left), 14 (upper right), 15 (lower left) and 16 (lower right) docked to the binding site.

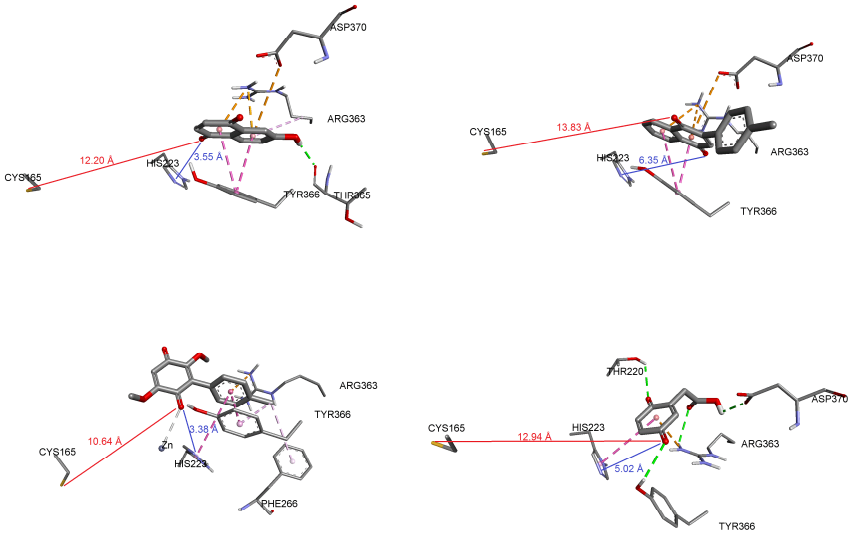

Figure 11. Molecules 17 (upper left), 18 (upper right), 19 (lower left) and 20 (lower right) docked to the binding site.

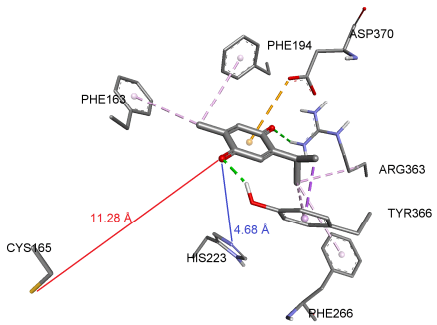

Figure 12. Molecule 21 docked to the binding site.

We can see in all the figures that Cys-165 is very far from the docked molecules (between 9.75 and 15.41 Å), while His-223 is very close to them (between 3.38 and 7.01 Å). On this basis we suggest that His-223 could be the target for covalent bond formation with 1,4-BQs and 1,4-NQs. But we must remember that this controversy can be solved only through more experimental work.

In conclusion, we have shown that in a group of 1,4BQs and 1,4NQs there is a good relationship between the variation of the rate constant to form the inactivated enzyme-ligand complex and the variation of the value of various local atomic reactivity indices. Also, docking studies that use rigid targets seem to be conceptually poor [38, 39, 48]. Allowing conformational flexibility to the residues forming the binding site should provide a closer view of what really happens during the ligand-site interaction. We have proposed that His-223 and not Cys-165 is the target for covalent bond formation.

APPENDIX.

During our research we carefully analyzed a paper of Louis Hammett and Helmuth Pfluger entitled "*The Rate of Addition of Methyl Esters to Trimethylamine*" [49]. As Shorter pointed out, "*this was Hammett's first research involving rate measurements. The experimental procedures are described in detail and the work was manifestly carried out very carefully. The selection of a temperature about 35 °C above the normal boiling point of methanol necessitated the use of sealed ampoules throughout the work. The progress of the reaction was followed by determining the concentration of trimethylamine which remained after definite intervals of time. Even at the elevated temperature used, the experiments with the less reactive esters lasted one to two weeks, and with the more reactive esters, a day or two. Good second-order kinetics were usually obtained*" [50]. During one interview Hammett said that "*the Pfluger paper on the addition of methyl esters to trimethylamine, I think, was a very important piece of work*" [51]. Fig. 1 of that paper reports a linear relationship between the logarithm of the rate constant ($K_{alkylation}$) and the logarithm of the dissociation constant of the corresponding acid at either 100 or 99°. The authors stated that the associated equation "*fits these data excellently except in the case of o-nitrobenzoate. The deviation of almost 0.3 units in this case requires further investigation*" [49]. A new search of the literature showed that this point never was clarified. We decided to repeat the calculations step by step founding that the authors did not calculate correctly the values for *o*-nitrobenzoic. Figure 13 shows the corrected plot.

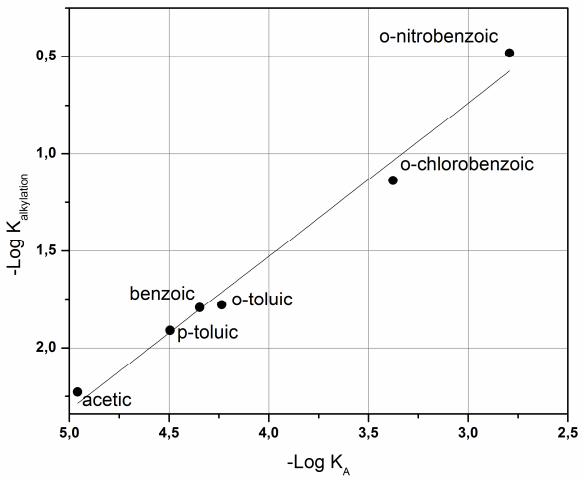

Figure 13. Plot of the logarithm of the rate constant against the logarithm of the dissociation constant of the corresponding acid.

The associated straight line is $\log(K_{alkylation}) = 0.79\log(K_A) + 1.63$ (r=0.99, SD= 0.08). We can see that now the plot has not points deserving "*more research*". One of us (J.S.G-J), following the rules of the scientific method, sent a note with the above corrections to the journal were the original paper appeared. Part of the editor's answer was that "*we do publish Addition/Corrections if errors of consequence are detected in a published paper. However, Addition/Corrections may only be submitted by the corresponding author of the original paper*". Considering that the article is of year 1933 and both authors are deceased as far as we know, the last phrase of the editor does not deserve more comments. The strength of the scientific method is found not so much in its capacity to detect truths, but in its ability to identify errors (and report them). This last ability seems to be lost in this case.

REFERENCES

[1] IW Fong; K Alibek, *Bioterrorism and infectious agents: a new dilemma for the 21st century*, Springer, Dordrecht ; New York, **2009**.
[2] P Gopalakrishnakone, *Biological toxins and bioterrorism*, Springer, Heidelberg, **2015**.
[3] R Katz; RA Zilinskas, *Encyclopedia of bioterrorism defense*, Wiley-Blackwell, Hoboken, N.J., **2011**.
[4] JR Ryan; J Glarum, *Biosecurity and bioterrorism: containing and preventing biological threats*, Butterworth-Heinemann, Amsterdam ; Boston, **2008**.
[5] D Emmeluth, *Botulism*, Chelsea House, New York, **2010**.
[6] KA Foster, *Molecular aspects of botulinum neurotoxin*, Springer, Heidelberg, **2014**.
[7] PT Bremer; MS Hixon; KD Janda, *Bioorg. Med. Chem.*, **2014**, 22, 3971-3981.
[8] JS Gómez Jeria, *Boll. Chim. Farmac.*, **1982**, 121, 619-625.
[9] JS Gómez-Jeria, *Int. J. Quant. Chem.*, **1983**, 23, 1969-1972.
[10] JS Gómez-Jeria, "Modeling the Drug-Receptor Interaction in Quantum Pharmacology," in *Molecules in Physics, Chemistry, and Biology*, J. Maruani Ed., vol. 4, pp. 215-231, Springer Netherlands, **1989**.
[11] JS Gómez-Jeria; M Ojeda-Vergara, *J. Chil. Chem. Soc.*, **2003**, 48, 119-124.
[12] JS Gómez-Jeria, *Elements of Molecular Electronic Pharmacology (in Spanish)*, Ediciones Sokar, Santiago de Chile, **2013**.
[13] JS Gómez-Jeria, *Canad. Chem. Trans.*, **2013**, 1, 25-55.
[14] C Barahona-Urbina; S Nuñez-Gonzalez; JS Gómez-Jeria, *J. Chil. Chem. Soc.*, **2012**, 57, 1497-1503.
[15] T Bruna-Larenas; JS Gómez-Jeria, *Int. J. Med. Chem.*, **2012**, 2012 Article ID 682495, 1-16.
[16] JS Gómez-Jeria; M Flores-Catalán, *Canad. Chem. Trans.*, **2013**, 1, 215-237.
[17] A Paz de la Vega; DA Alarcón; JS Gómez-Jeria, *J. Chil. Chem. Soc.*, **2013**, 58, 1842-1851.
[18] I Reyes-Díaz; JS Gómez-Jeria, *J. Comput. Methods Drug Des.*, **2013**, 3, 11-21.
[19] F Gatica-Díaz; JS Gómez-Jeria, *J. Comput. Methods Drug Des.*, **2014**, 4, 79-120.
[20] JS Gómez-Jeria, *Int. Res. J. Pure App. Chem.*, **2014**, 4, 270-291.
[21] JS Gómez-Jeria, *Der Pharm. Lett.*, **2014**, 6., 95-104.
[22] JS Gómez-Jeria, *Brit. Microbiol. Res. J.*, **2014**, 4, 968-987.
[23] JS Gómez-Jeria, *SOP Trans. Phys. Chem.*, **2014**, 1, 10-28.
[24] JS Gómez-Jeria, *Der Pharma Chem.*, **2014**, 6, 64-77.
[25] JS Gómez-Jeria, *Res. J. Pharmac. Biol. Chem. Sci.*, **2014**, 5, 2124-2142.
[26] JS Gómez-Jeria, *J. Comput. Methods Drug Des.*, **2014**, 4, 32-44.
[27] JS Gómez-Jeria, *Res. J. Pharmac. Biol. Chem. Sci.*, **2014**, 5, 424-436.
[28] JS Gómez-Jeria, *J. Comput. Methods Drug Des.*, **2014**, 4, 38-47.
[29] JS Gómez-Jeria, *Res. J. Pharmac. Biol. Chem. Sci.*, **2014**, 5, 780-792.
[30] JS Gómez-Jeria; J Molina-Hidalgo, *J. Comput. Methods Drug Des.*, **2014**, 4, 1-9.
[31] JS Gómez-Jeria; J Valdebenito-Gamboa, *Der Pharma Chem.*, **2014**, 6, 383-406.
[32] D Muñoz-Gacitúa; JS Gómez-Jeria, *J. Comput. Methods Drug Des.*, **2014**, 4, 33-47.
[33] D Muñoz-Gacitúa; JS Gómez-Jeria, *J. Comput. Methods Drug Des.*, **2014**, 4, 48-63.
[34] DI Pino-Ramírez; JS Gómez-Jeria, *Amer. Chem. Sci. J.*, **2014**, 4, 554-575.
[35] F Salgado-Valdés; JS Gómez-Jeria, *J. Quant. Chem.*, **2014**, 2014 Article ID 431432, 1-15.
[36] R Solís-Gutiérrez; JS Gómez-Jeria, *Res. J. Pharmac. Biol. Chem. Sci.*, **2014**, 5, 1401-1416.
[37] JS Gómez-Jeria; A Robles-Navarro, *Res. J. Pharmac. Biol. Chem. Sci.*, **2015**, 6, 1337-1351.
[38] JS Gómez-Jeria; A Robles-Navarro, *Der Pharma Chem.*, **2015**, 7, 243-269.
[39] MS Leal; A Robles-Navarro; JS Gómez-Jeria, *Der Pharm. Lett.*, **2015**, 7, 54-66.
[40] MJ Frisch; GW Trucks; HB Schlegel; GE Scuseria; MA Robb, et al., G03 Rev. E.01, Gaussian, Pittsburgh, PA, USA, 2007.
[41] JS Gómez-Jeria, D-Cent-QSAR: A program to generate Local Atomic Reactivity Indices from Gaussian log files. 1.0, Santiago, Chile, **2014**.
[42] JS Gómez-Jeria, *J. Chil. Chem. Soc.*, **2009**, 54, 482-485.
[43] Statsoft, Statistica 8.0, 2300 East 14 th St. Tulsa, OK 74104, USA, **1984-2007**.

[44] O Trott; AJ Olson, *J. Comput. Chem.*, **2010**, 31, 455-461.
[45] Accelrys SoftwareInc., Discovery Studio Visualizer 4.1, Accelrys Software Inc., San Diego, CA, USA, **2013**.
[46] Y Kumagai; Y Shinkai; T Miura; AK Cho, *Ann. Rev. Pharmacol. Toxicol.*, **2012**, 52, 221-247.
[47] AA Fisher; MT Labenski; S Malladi; JD Chapman; SB Bratton, et al., *Toxicol. Sci.*, **2011**,
[48] JS Gómez-Jeria; A Robles-Navarro, *in press*, **2015**,
[49] LP Hammett; HL Pfluger, *J. Am. Chem. Soc.*, **1933**, 55, 4079-4089.
[50] J Shorter, *Chem. Listy*, **2000**, 94, 210-214.
[51] American Institute of Physics, "Interview with Dr. Louis Hammett by Leon Gortler in Medford, New Jersey, May 22, 1978," http://www.aip.org/history/ohilist/4654_2.html, **1978**.